Operating Strategies for a GB Integrated Gas and Electricity Network Considering the Uncertainty in Wind Power Forecasts

Meysam Qadrdan, *Member, IEEE*, Jianzhong Wu, *Member, IEEE*, Nick Jenkins, *Fellow, IEEE*, and Janaka Ekanayake, *Senior Member, IEEE*

***Abstract*—In many power systems, in particular in Great Britain (GB), significant wind generation is anticipated and gas-fired generation will continue to play an important role. Gas-fired generating units act as a link between the gas and electricity networks. The variability of wind power is, therefore, transferred to the gas network by influencing the gas demand for electricity generation. Operation of a GB integrated gas and electricity network considering the uncertainty in wind power forecast was investigated using three operational planning methods: deterministic, two-stage stochastic programming, and multistage stochastic programming. These methods were benchmarked against a perfect foresight model which has no uncertainty associated with the wind power forecast. In all the methods, thermal generators were controlled through an integrated unit commitment and economic dispatch algorithm that used mixed integer programming. The nonlinear characteristics of the gas network, including the gas flow along pipes and the operation of compressors, were taken into account and the resultant nonlinear problem was solved using successive linear programming. The operational strategies determined by the stochastic programming methods showed reductions of the operational costs compared to the solution of the deterministic method by almost 1%. Also, using the stochastic programming methods to schedule the thermal units was shown to make a better use of pumped storage plants to mitigate the variability and uncertainty of the net demand.**

***Index Terms*—Integrated gas and electricity network, stochastic programming, wind power forecast uncertainty.**

NOMENCLATURE

Constants

R Gas constant for natural gas (518 J/kgK).

Z Gas compressibility factor (0.95).

Re Reynolds number.

Superscripts

ι Gas injection.

ω Gas withdrawal.

w Wind power.

sp Spot price.

ue Unserved electricity.

ug Unserved gas.

su Startup.

sd Shutdown.

f Fuel cost of power generation.

var Variable (nonfuel) cost of power generation.

s Scenarios.

av Average value of a variable.

n Standard condition for gas.

Subscripts

t Time.

u Gas storage facility.

b Electrical busbar.

i Power generator.

m Gas node.

q Gas pipe.

g Gas terminal.

c Gas compressor.

l Transmission line.

k Thermal generator.

Parameters

A Cross-sectional area of a pipe (m^2).

D Diameter of a pipe (m).

π The probability of a wind power forecast scenario (%).

C Cost (£).

Temp Gas temperature (K).

ρ Gas density, assuming standard conditions ($\mathrm{kg/m}^3$).

γ Friction factor in a pipe.

V Volume of a pipe (m^3).

α Polytropic exponent of a gas compressor (1.27).

β Gas turbine fuel rate coefficient of a compressor ($0.084\ \mathrm{m}^3/\mathrm{MJ}$).

Manuscript received January 19, 2013; revised June 06, 2013; accepted July 21, 2013. Date of publication September 05, 2013; date of current version December 12, 2013. The research reported in this paper was part of the U.K. Infrastructure Transitions Research Consortium (ITRC) funded by the Engineering and Physical Sciences Research Council under Programme Grant EP/I01344X/1.

The authors are with the Electrical and Electronic Engineering Department, Cardiff University, Cardiff, CF24 3AA, U.K.

Color versions of one or more of the figures in this paper are available online at http://ieeexplore.ieee.org.

Digital Object Identifier 10.1109/TSTE.2013.2274818

η	Efficiency (%).
$\mathbb{E}(.)$	Expected value of a function.
$\overline{P}$	Maximum generation capacity of a unit (MW).
$\underline{P}$	Minimum power generation of a unit (MW).
TC	Cool-down time (h).
C_{TC}	Maximum cold startup cost $(£)$.
rw	Percentage of wind generation contributing to spinning reserve requirements (%).
$\underline{r}$	Minimum reserve requirement to support generators outages and forecast errors in electricity demand (MW).
UT	Minimum uptime for thermal units (h).
DT	Minimum downtime for thermal units (h).
$\overline{R}$	Maximum power ramp-up (MW/h).
$\underline{R}$	Maximum power ramp-down (MW/h).
CPR	Compressor pressure ratio.
H	Gas heating value (39 MJ/m^3).

Variables

P	Electrical power (MW).
p	Gas pressure (Pascal).
Q	Volumetric gas flow rate $(\mathrm{m}^3/\mathrm{s})$.
$\partial\mathrm{LP}$	Linepack changes $(\mathrm{m}^3/\mathrm{s})$.
LP	Gas linepack (m^3).
τ	Amount of gas tapped by a compressor $(\mathrm{m}^3/\mathrm{s})$.
S	Gas storage level (m^3).
ν	ON/OFF state of a thermal unit (1/0).
r	Spinning reserve (MW).
E	Stored energy in a pumped storage unit (MWh).

I. Introduction

AS THE fraction of wind power generation in a power system increases, it becomes important to take account of the wind variability and the uncertainty in the forecasts of wind power.

Several studies have examined the effect of uncertainty in wind power forecasts on unit commitment. Carpentier *et al.* [1] presented a stochastic decomposition method to deal with large-scale unit commitment. Wang *et al.* [2] presented a security-constrained unit commitment algorithm to take into account the intermittency and uncertainty of wind power generation. In [3], a particle swarm optimization technique was used to solve a stochastic cost model considering load and wind power uncertainties. Gonzalez *et al.* [4] formulated a two-stage stochastic programming model to optimize the combined operation of a wind farm and a pumped storage facility in a market environment with wind generation and electricity price uncertainties. Bouffard and Galiana [5] formulated a short-term forward electricity market-clearing model for nondispatchable and variable wind power generation sources. Tuohy *et al.* [6] examined the effects of uncertain wind and load on the unit commitment and dispatch of power systems with high levels of wind power generation. Methaprayoon *et al.* [7] developed an artificial neural network model to generate uncertain wind power forecasts. This model was integrated into unit commitment scheduling.

Given the strong linkage between gas and electricity networks in Great Britain (GB), the ability of the power system to meet the uncertain net demand is affected by performance of the gas network [8]–[10]. Although the storage capacity of the gas transmission network provides a buffer to compensate for demand variations to a degree, gas supply and pressure in the network need to be adjusted to cope with more extreme cases. Therefore, modeling the integrated network using stochastic programming allows improved unit scheduling decisions to be made.

An integrated model of gas and electricity networks was developed to take into account the uncertainty in wind power forecast and fuel availability to gas-fired generators. The uncertainty in the forecasts of electricity demand is significantly less than that of wind power; therefore, in this research, only the uncertainty of wind power forecasts are considered.

II. Operational Planning Methods to Address Uncertainty in Wind Power Forecasts

The uncertainty in wind power forecast was addressed using three operational planning methods: deterministic (DM), two-stage stochastic programming (TSM), and multistage stochastic programming (MSM). These methods were benchmarked against a perfect foresight method (PFM) which has no uncertainty associated with the wind power forecast. The fundamental theories of stochastic programming are described within [11].

Deterministic Method (DM): In the deterministic method, the decision on the day-ahead unit commitment was made using a single point wind power forecast. In order to compensate for any deviation of the wind power outturn from the single point forecast, a predetermined level of spinning reserve was maintained. Then given the committed units, economic dispatch decisions were determined for possible outturns of wind power (forecast scenarios). The reason for using the wind power forecast scenarios in making economic dispatch decisions is to take into account different possibilities of wind power outturn when the expected cost of operating the system is calculated.

Two-Stage Stochastic Method (TSM): In the two-stage stochastic programming method, probabilistic wind power forecast scenarios were used. In the first stage of decision making, a unit commitment decision was made for the whole operating horizon (day-ahead scheduling) considering different possibilities of wind power outturn. Then in the second stage, economic dispatch decisions were made for the possible outturns of wind power.

Multistage Stochastic Method (MSM): In the multistage stochastic programming method, probabilistic wind power forecast scenarios were used. The MSM allows for making multiple day-ahead unit commitment decisions. There is a day-ahead unit commitment decision for each forecast scenario. Nonanticipativity constraints ensure that the decisions for different forecast scenarios are the same for the period when the forecast scenarios

TABLE I
WIND POWER FORECAST DATA USED BY OPERATIONAL PLANNING METHODS FOR UNIT COMMITMENT AND ECONOMIC DISPATCH DECISION-MAKING PROCESS

Operational planning methods	Input/Output	Unit commitment	Economic dispatch	Predetermined reserve for wind power
PFM	Input	Single wind power forecast	Single wind power forecast	No
	Output	Single unit commitment solution	Single economic dispatch solution	
DM	Input	Single wind power forecast	Probabilistic wind power forecasts	Yes
	Output	Single unit commitment solution	Multiple economic dispatch solutions	
TSM	Input	Probabilistic wind power forecasts	Probabilistic wind power forecasts	No
	Output	Single unit commitment solution	Multiple economic dispatch solutions	
MSM	Input	Probabilistic wind power forecasts	Probabilistic wind power forecasts	No
	Output	Multiple unit commitment solutions	Multiple economic dispatch solutions	

have not branched out yet. Therefore, in the MSM for each wind power forecast scenario, a unit commitment and an economic dispatch decision were made. In practice, when the uncertainties associated with wind power forecast are gradually observed, the appropriate unit commitment and economic dispatch decisions, that have already been made, will be adjusted.

The main difference between the above methods is the way that unit commitment and economic dispatch decisions were made. Given a single wind power forecast and probabilistic wind power forecast scenarios, the decision-making process of a system operator, in the presence of the uncertainty in wind power, was modeled using different operational planning methods. The type of wind power forecast (single forecast and probabilistic forecast scenarios) used by the above operational planning methods, along with the form of unit commitment and economic dispatch solutions (single set of solution and multiple sets of solutions), are shown in Table I.

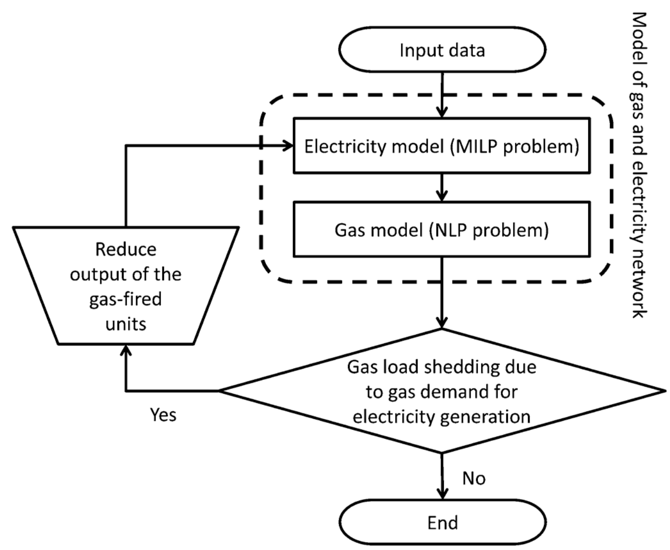

Fig. 1. Structure of the integrated gas and electricity network model.

III. MODELING OF THE GB INTEGRATED GAS AND ELECTRICITY NETWORK

In this section, the modeling of the GB integrated gas and electricity network is presented. The modeling was implemented using the Fico Xpress Optimization suite. The structure used for the model is shown in Fig. 1. This structure consists of two separate parts: a mixed integer linear programming (MILP) model for the electricity network (including unit commitment, economic dispatch, and load flow) and a nonlinear programming (NLP) model for the gas network. The electricity network model is solved first using a branch and bound algorithm. The results are used to determine the gas demand for electricity generation for use within the gas model. The gas network problem is then solved using successive linear programming (SLP).

The solution of the gas network model is then checked to make sure there is no gas load shedding due to additional gas demand from gas-fired generators. In the case when gas load shedding does occur, a heuristic method is used to constrain the power output from the gas-fired generators, and the electricity and gas models are run repeatedly until a feasible solution is obtained. From the optimization perspective, the solution is not globally optimal, since the optimization problems for gas and electricity networks are not treated as one problem. However, the structure replicates the way that the GB gas and electricity networks are operated. In practice, operation of these networks are optimized separately with the gas network supplying gas to gas-fired plants until it is not feasible to do so.

The mixed integer linear optimization problem of the electricity network was solved using a branch and bound algorithm. The nonlinear optimization problem of the gas network was solved using successive linear programming (SLP).

A. Objective Function

Equation (1) shows the expected operational cost of the electricity network which consists of fuel and variable costs of power generation, cost of unserved electricity, startup and shutdown costs of thermal generating units. Equation (2) shows the expected operational cost of the gas network which consists of cost of gas supply from terminals, costs of gas injection into and withdrawal from gas storage facilities, cost of gas provided by linepack, and cost of unserved gas.

The objective function is to minimize the summation of the expected costs of gas and electricity networks (3):

$$f^{\mathrm{elec}}(s)=\sum_s \pi^s \times \sum_t \left\{ \sum_i \left(C^f_{i,t} + C^{\mathrm{var}}_i \right) P^s_{i,t} + \sum_b C^{\mathrm{ue}} P^{\mathrm{ue},s}_{b,t} + \sum_k C^{\mathrm{su},s}_{k,t} + \sum_k C^{\mathrm{sd},s}_{k,t} \right\} \quad (1)$$

$$f^{\mathrm{gas}}(s)=\sum_s \pi^s \times \sum_t \left\{ \sum_g C^{\mathrm{gas}}_{g,t} Q^s_{g,t} + \sum_u \left(C^{\iota} Q^{\iota,s}_{u,t} + C^{\omega} Q^{\omega,s}_{u,t} \right) \right.$$

$$\left. +\sum_q C_t^{\mathrm{gas,sp}} \partial \mathrm{LP}_{q,t}^s + \sum_m C^{\mathrm{ug}} Q_{m,t}^{\mathrm{ug},s} \right\} \tag{2}$$

$$f = \min(f^{\mathrm{elec}} + f^{\mathrm{gas}}). \tag{3}$$

Superscript s represents scenarios of the probabilistic wind power forecast.

B. Electricity Network

1) Power Balance Constraint: The power balance constraint requires that the total generation is equal to the total demand minus the load shed at each time step

$$\sum_i P_{i,t}^s = \sum_b P_{b,t}^{\mathrm{demand}} - \sum_b P_{b,t}^{s,\mathrm{ue}}. \tag{4}$$

2) Power Generation: Electrical power generation is kept within the physical limits of the generating units

$$\underline{P}_i \leq P_{i,t}^s \leq \overline{P}_i. \tag{5}$$

3) Ramp Rate Constraints: Power generators cannot ramp up or ramp down instantaneously. Therefore, the following constraints were imposed within the model:

$$P_{i,t}^s - P_{i,t-1}^s \leq \overline{R}_i \tag{6}$$

$$P_{i,t-1}^s - P_{i,t}^s \leq \underline{R}_i. \tag{7}$$

4) Power Transmission: The electricity network was modeled using a dc power flow [12], [13]. The power transmission along each line was constrained by defining a maximum transmission capacity

$$P_{l,t}^s \leq P_l^{\max}. \tag{8}$$

5) Startup Cost: The startup cost of a thermal generating unit depends on its downtime; this will vary from a maximum cold start value to a much smaller value when the generating unit is still relatively close to its operating temperature. A typical startup cost function for a thermal generating unit has an exponential form [14]. Because the time step in this study is discrete, the exponential startup cost was approximated by using the stepwise function shown by Fig. 2.

The startup cost of thermal generating units was modeled using (9), as follows [15]:

$$C_{k,t}^{\mathrm{su},s} = \max_{T'=1:\mathrm{TC}_k} C_{k,T'} \times \left(\nu_{k,t}^s - \sum_{t'=1}^{T'} \nu_{k,t-t'}^s \right) \tag{9}$$

where $0 < C_{k,1} < \cdots < C_{k,\mathrm{TC}_k}$ are fixed cost coefficients derived from the stepwise form of the startup cost function. The discretized startup costs for thermal generating units are shown in Table II, and were assumed to be the same for different technologies and capacities.

6) Shutdown Cost: A constant shutdown cost of $(£)1000$ [16] was assumed for thermal generating units

$$C_t^{\mathrm{sd},s} = \max\left\{ C^{\mathrm{sd}} \left[\nu_{k,t-1}^s - \nu_{k,t}^s \right], 0 \right\} \tag{10}$$

to model the waste of fuel when a unit is brought offline [14].

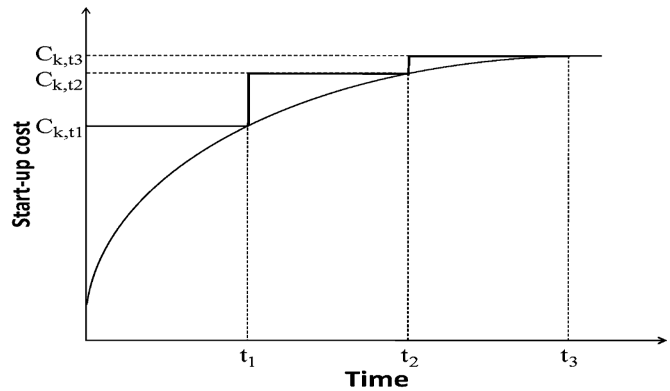

Fig. 2. Discretized startup cost for thermal generating units. The horizontal axes shows time length in which a thermal generating unit remained OFF, before starting up.

TABLE II
DISCRETIZED STARTUP COSTS FOR THERMAL GENERATING UNITS [16]

Off-line time (h)	1	2	3	4	5	6
Cost (£)	1334	2748	3868	4598	5167	5475
Off-line time (h) Cont.	7	8	9	10		
Cost (£) Cont.	5575	5644	5738	5820		

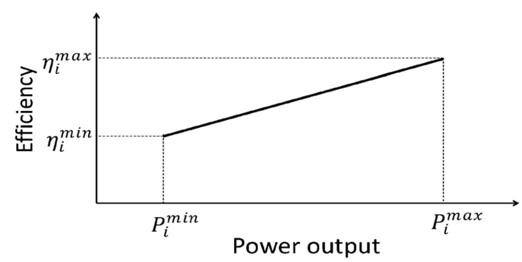

Fig. 3. Linear approximation of part-load efficiency for thermal generating units.

7) Part-Load Efficiency: The impact of part-load efficiency on the generation cost of thermal generating units was taken into account ($fuel \propto 1/\eta$). For the sake of simplicity, the part-load efficiency was modeled using a linear approximation depicted in Fig. 3 [17].

It was assumed that efficiency of thermal generating units vary with their power output. Minimum and maximum efficiencies of different thermal generating units are shown in Table III.

8) Spinning Reserve: Spinning reserve is used to control the frequency and to maintain the balance between power demand and supply at all times. The amount of available spinning reserve is equal to the unused capacity of synchronized generators which can be dispatched immediately upon decision of the system operator. The minimum spinning reserve requirement ($\underline{r}$) varies in different systems. In conventional systems, the required amount of spinning reserve is usually equal to the capacity of the largest generator, or a certain percentage of the peak load.

When using a deterministic approach, a higher level of reserve is required to deal with uncertainties within the wind power forecast. The reserve requirement equation shown in (11) consists of two parts representing reserve requirement for generating unit outages and uncertainty in wind forecast:

$$r_t = \sum_k r_{k,t} \geq (\underline{r} + rw \times P_t^w) \tag{11}$$

TABLE III
EFFICIENCIES [17] AND COSTS [21] FOR DIFFERENT GENERATION UNITS. *COMBINED CYCLE GAS TURBINE. **OPEN CYCLE GAS TURBINE

Generating units	η^{min}	η^{max}	C^{f}(£/MWh)	C^{var}(£/MWh)
Coal	35%	45%	19.9	2.2
CCGT*	50%	60%	50.9	2.3
OCGT**	30%	40%	66.3	1.5
Nuclear	-	-	5.2	1.8
Pumped storage	80	80	-	3
Biomass	35	45	70	2.2

TABLE IV
MINIMUM UPTIME/DOWNTIME, COOL-DOWN TIME, AND RAMP UP/DOWN DATA FOR DIFFERENT THERMAL GENERATING UNITS [17]

Generating units	UT(h)	DT(h)	TC(h)	$\overline{\mathbf{R}}$(MW/h)	$\underline{\mathbf{R}}$(MW/h)
Coal	8	4	8	200	200
CCGT	4	4	4	250	250
OCGT	1	1	2	300	300
Biomass	8	4	8	200	200

where

$$r_{k,t} = \nu_{k,t} \times (\overline{P}_k - P_{k,t}). \tag{12}$$

In the stochastic programming methods, the uncertainties of wind forecasts are taken into account implicitly through representative wind forecast scenarios. Therefore, the reserve requirement in the stochastic programming methods was considered only for generating units outages where $r_t^s = \sum_k r_{k,t}^s \geq \underline{r}$.

9) Minimum Uptime and Downtime: When a thermal generating unit is up or down it must remain so for minimum UT and DT periods, respectively. Minimum up/down constraints were implemented using [15]

$$\nu_{k,t'}^s - \nu_{k,t'-1}^s \leq \nu_{k,t}^s, \quad t' = [t - \mathrm{UT}_k + 1, t-1] \tag{13}$$
$$\nu_{k,t'-1}^s - \nu_{k,t'}^s \leq 1 - \nu_{k,t}^s, \quad t' = [t - \mathrm{DT}_k + 1, t-1]. \tag{14}$$

Minimum up/down time as well as ramp up/down data for different thermal generating units are shown in Table IV.

10) Pumped Storage Plant: The dynamic behavior of pumped storage units was modeled by defining the storage level of equivalent electrical energy

$$E_{i,t}^s = E_{i,t-1}^s + \left(\eta^{\mathrm{pump}} \times P_{i,t}^{\mathrm{pump},s} - P_{i,t}^s\right) \times ts \tag{15}$$

and by the constraints upon pumped storage power generation

$$P_{i,t}^s \times ts \leq \min\left(\overline{P}_i \times ts, E_{i,t-1}^s\right) \tag{16}$$

where η^{pump} is pumping efficiency, $P_{i,t}^{\mathrm{pump}}$ is pumping power, and ts is the length of time step which is one hour in this study.

C. Gas Network

The components of the gas network modeled were the pipelines, compressors, storage facilities, and gas terminals. More details about modeling of a gas network can be found in [18] and [19]. The balance of total gas supply and demand at each time step was satisfied

$$\sum_g Q_{g,t} + \sum_u Q_{u,t}^{\omega} - \sum_u Q_{u,t}^{\iota} = \sum_c \tau_{c,t} + \sum_m Q_{m,t}^{demand} - \sum_m Q_{m,t}^{\mathrm{ug}}. \tag{17}$$

1) Gas Flow in a Pipe: The gas flow rate within each pipe was determined by the pressure difference between upstream and downstream nodes

$$\frac{p_{q,\mathrm{up}}^s - p_{q,\mathrm{down}}^s}{L_q} = -\frac{2ZR\mathrm{Temp}\gamma(\rho^n)^2\left(Q_{q,t}^{n,s,\mathrm{av}}\right)\left|Q_{q,t}^{n,s,\mathrm{av}}\right|}{(A_q)^2 D_q p_q^{s,\mathrm{av}}} \tag{18}$$

where subscripts *up* and *down* refer to the upstream and downstream nodes of pipe q, and L is length of the pipe. The "Panhandle A" implementation of the friction factor (γ) for high pressure networks ($p > 7 \times 10^5$ Pascal) was used.

2) Gas Storage: The amount of gas stored in a storage facility at each time step was constrained using

$$S_{u,t}^s = S_{u,t-1}^s - Q_{u,t}^{\omega,s} + Q_{u,t}^{\iota,s} \tag{19}$$

where $Q_{u,t}^{\omega}$ and $Q_{u,t}^{\iota}$ are gas withdrawal and injection, and constrained through (20) and (21), respectively:

$$0 < Q_{u,t}^{\omega,s} \leq Q_{u,t}^{\omega,\max} \tag{20}$$
$$0 < Q_{u,t}^{\iota,s} \leq Q_{u,t}^{\iota,\max}. \tag{21}$$

3) Gas Compressor: Compressors are used in the gas transmission network to boost network pressure and thus ensure gas delivery to each demand node. The power required by the compressor prime-mover is calculated by [18]

$$P_{c,t}^s = \frac{Q_{c,t}^{n,s}\alpha}{\eta_c(\alpha-1)}\left[\left(\frac{p_{c,t}^{\mathrm{out},s}}{p_{c,t}^{\mathrm{in},s}}\right)^{\frac{(\alpha-1)}{\alpha}} - 1\right] \tag{22}$$

where superscripts *in* and *out* refer to the inlet and outlet of the compressor.

In practice, performance of a compressor is restricted by the pressure ratio (23), flow capacity (24), and maximum power (25):

$$1 \leq \frac{p_{c,t}^{\mathrm{out},s}}{p_{c,t}^{\mathrm{in},s}} \leq \mathrm{CPR}^{\max} \tag{23}$$
$$Q_{c,t}^{n,s} \leq Q_c^{n,\max} \tag{24}$$
$$P_{c,t}^s \leq P_c^{\max}. \tag{25}$$

The amount of gas tapped by the compressor as fuel was approximated by [20]

$$\tau_{c,t}^s = \beta P_{c,t}^s. \tag{26}$$

4) Gas Network Linepack: Linepack refers to the volume of gas stored within a pipe and is a key factor that affects the ability of a network to supply gas to demand nodes, i.e., a highly packed pipe allows fluctuations in demand to be met locally as gas supply from a distant source will take time (typically hours) to reach its intended destination.

The linepack of a pipe when the gas flow is in steady state is calculated using

$$\mathrm{LP}_{q,t}^{s} = V_t^{n,s} = \frac{p_{q,t}^{\mathrm{av},s} V_q}{\rho^n Z R \mathrm{Temp}^n}. \tag{27}$$

This illustrates that pipe linepack is proportional to the average pressure within the pipe, so that an increase of average pressure will increase the linepack and vice versa.

The gas density ρ^n and gas temperature Temp^n under standard condition are 0.713 kg/m^3 and 288 K. Under dynamic situations, the gas flow into and out of a pipe fluctuates with changing supply and demand. According to the law of conservation of mass, the change of total gas volume is equal to the difference between the flow into and out of the pipe. Thus, (27) is changed to

$$\mathrm{LP}_{q,t}^{s} = \mathrm{LP}_{q,t-1}^{s} + \int_{t-1}^{t} \left(Q_{q,t-1}^{n,s,\mathrm{in}} - Q_{q,t-1}^{n,s,\mathrm{out}} \right) dt \tag{28}$$

where the initial gas stored in the pipe (LP_0) is calculated by (27) in the steady state condition, and superscripts *in* and *out* refer to gas flows into and out of a pipe.

D. Linkage Between Gas and Electricity Networks

Gas turbine generators link the gas and electricity networks. For the gas network, a gas turbine was looked upon as a gas load. Its value depends on the power output of the gas turbine. In the electricity network, the gas turbine generator is a source. The relationship between the gas fuel flow and the real electrical power generated is expressed as

$$P_{i,t}^{s} = \eta_i Q_{i,t}^{s} H. \tag{29}$$

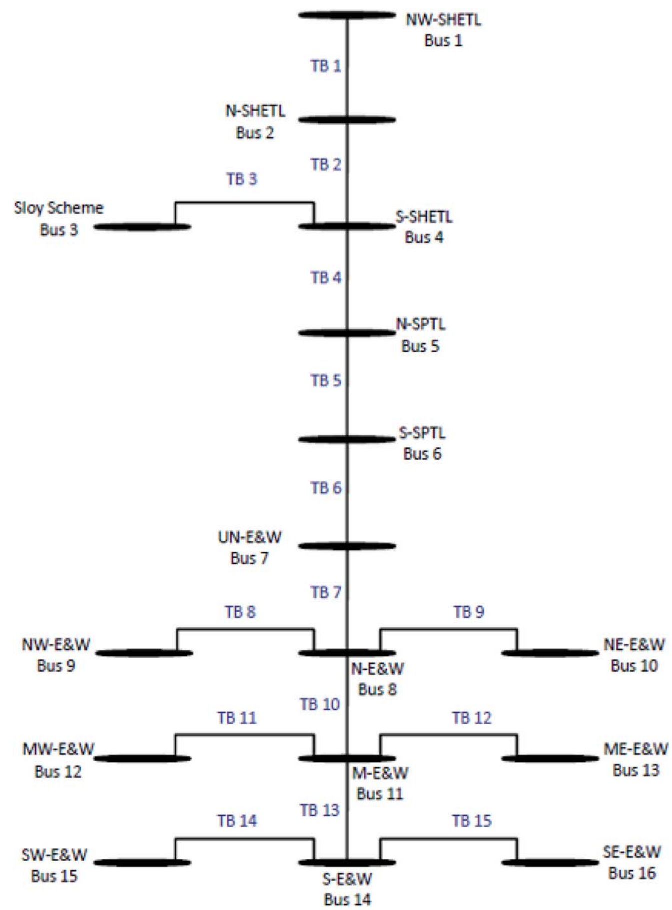

Fig. 4. GB 16 busbars electricity network. The load locates at all the busbars except Bus8 and Bus11.

IV. Case Study

A. Integrated Gas and Electricity Network

The simplified electricity and gas networks for GB, shown in Figs. 4 and 5, were modeled. The networks are linked together through gas-fired generators. Electricity and gas demand profile are shown in Figs. 6 and 7. The capacity of generating units at different locations are shown in Table V. The capacity of the power transmission lines are shown in Table VI.

The variable nonfuel operating cost and fuel cost for different technologies are shown in Table III. For thermal units, fuel cost data is based on their maximum efficiency.

B. Probabilistic Wind Power Forecasts

Different steps of producing probabilistic wind power forecasts are shown in Fig. 8. A single wind power forecast was calculated using the singular spectrum analysis (SSA) technique [24]. Given the forecast errors of the aggregated outputs of the wind farms [25], lower and upper limits were determined for each time step where the wind power outturn is most likely to fall within this range. Then a large number of random forecasts were generated within the lower and upper bounds using Monte Carlo simulation. It is worth noting that using the wider forecast error bounds improves the effectiveness of the stochastic programming methods.

It is very difficult to numerically obtain a solution for a stochastic optimization problem using the large number of wind power forecast scenarios [26]. On the other hand, a small number of wind power forecast scenarios provides less information about the possible wind power outturns. In order to address the above issues, a large number of wind power forecast scenarios were generated, and then a scenario reduction algorithm was applied to merge the forecast scenarios that are very close together.

Fig. 9 shows the result of applying the scenario reduction algorithm [27] on the 1000 initial scenarios. The initial 1000 scenarios were reduced to 5 representative forecast scenarios shown in Fig. 10.

The stability of the scenario reduction algorithm was tested using a two-stage stochastic model for electricity network. The model was run several times with different numbers of forecast scenarios and then the operational costs were compared (Fig. 11).

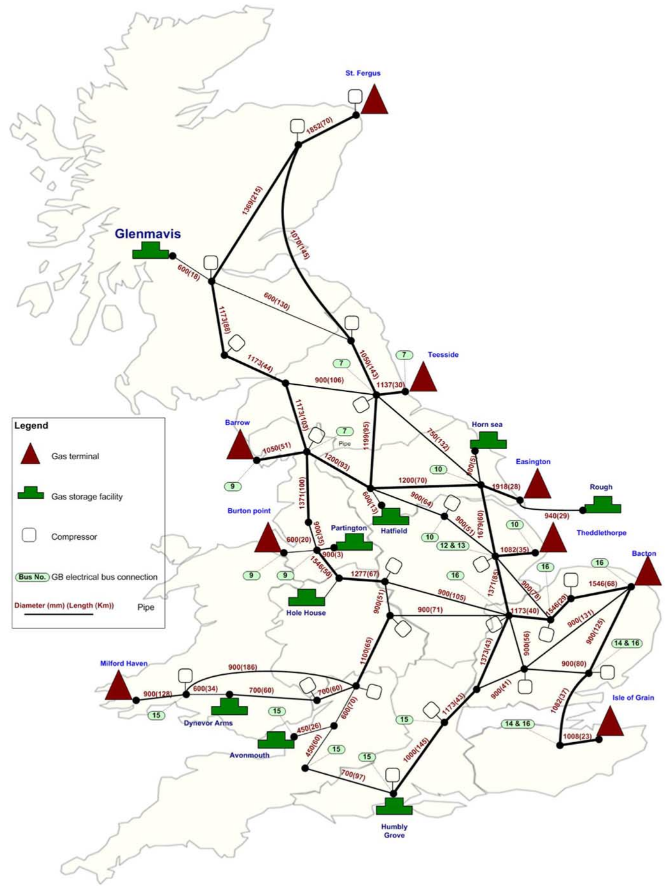

Fig. 5. Simplified GB gas network.

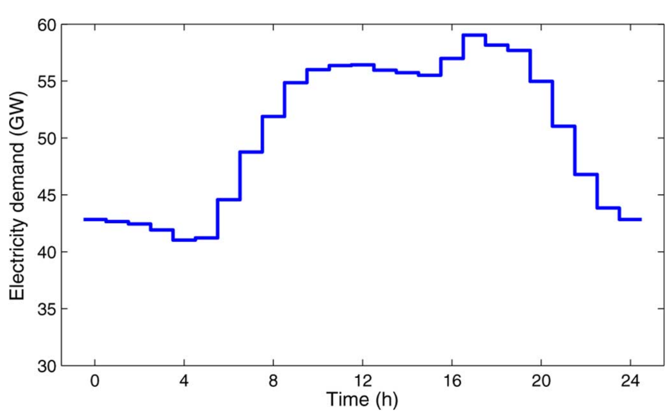

Fig. 6. Hourly electricity demand.

V. Results

A. Level of Spinning Reserve Used in the Deterministic Method (DM)

Dealing with the wind power uncertainty in the deterministic model necessitates the allocation of extra spinning reserve. Spinning reserve requirement for the single point wind power forecast (Fig. 10) for different values of rw [see (11)] are shown in Fig. 12. Impacts of applying different levels of spinning reserve on the operational cost of the electricity network are shown in Table VII.

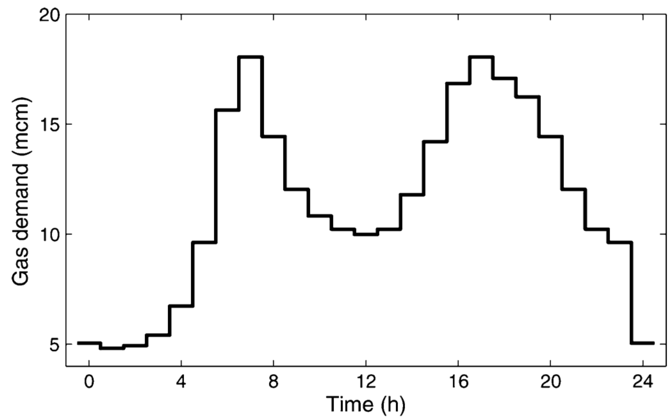

Fig. 7. Hourly gas demand for nonpower sectors.

TABLE V
Capacity of Power Generation at Different Locations (GW) [22]

Bus	Nuclear	Coal	Gas-fired	Wind	Inter-connector	Biomass	Hydro & pumped storage
Bus 1	-	-	-	3	-	-	0.9
Bus 2	-	-	1.64	3.9	-	-	-
Bus 3	-	-	-	-	-	-	0.25
Bus 4	-	-	-	-	-	-	0.23
Bus 5	-	1.3	-	2.25	-	0.05	0.44
Bus 6	1.2	-	0.34	2.25	-	0.05	0.03
Bus 7	1.2	2.93	3.21	2.365	-	0.3	-
Bus 8	-	-	-	-	-	-	-
Bus 9	2.22	1.48	4.26	4.24	0.87	-	2
Bus 10	-	4.7	4.7	2	-	-	-
Bus 11	-	-	-	-	-	-	-
Bus 12	-	2.97	2.85	0.98	-	-	-
Bus 13	-	1.8	3.88	4.5	-	-	-
Bus 14	-	-	2.43	1	-	-	-
Bus 15	-	3.16	5.88	1.5	-	0.4	-
Bus 16	2.28	1.46	5.71	1.46	3.33	-	-
Total	6.9	19.8	34.9	29.45	4.2	0.8	3.85

TABLE VI
Maximum Capacity of Interconnecting GB Transmission Circuit

GB transmission boundaries	TB1	TB2	TB3	TB4	TB5	TB6	TB7	TB8
Maximum capacity (GW)	1.6	2.8	0.5	3.3	5.15	5.8	7.5	0.65
GB transmission boundaries Cont.	TB9	TB10	TB11	TB12	TB13	TB14	TB15	
Maximum capacity (GW) Cont.	3.84	10.8	3.9	5.2	11.7	3.38	2.59	

In this research, 20% was considered to be an acceptable value for rw, due to providing reliable levels of reserve [28], [29] at reasonable operational costs. Therefore, results from the deterministic method with $rw = 20\%$ was compared to the results from the other methods.

B. Power Generation

Energy output from different types of generators for the perfect foresight method is shown in Fig. 13. Changes of electrical

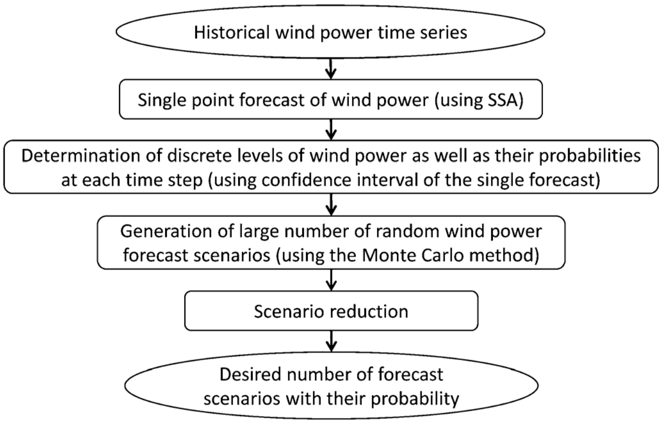

Fig. 8. Algorithm for producing probabilistic wind power forecasts.

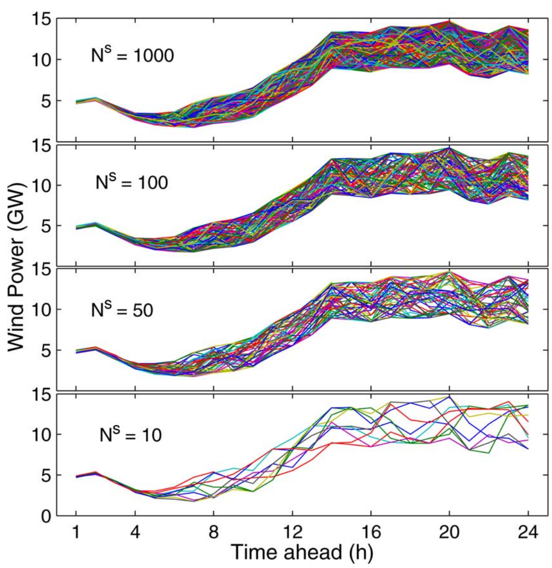

Fig. 9. Different number of wind power forecast scenarios derived by applying the scenario reduction algorithm on 1000 randomly generated scenarios. N^s is the number of wind power forecast scenarios.

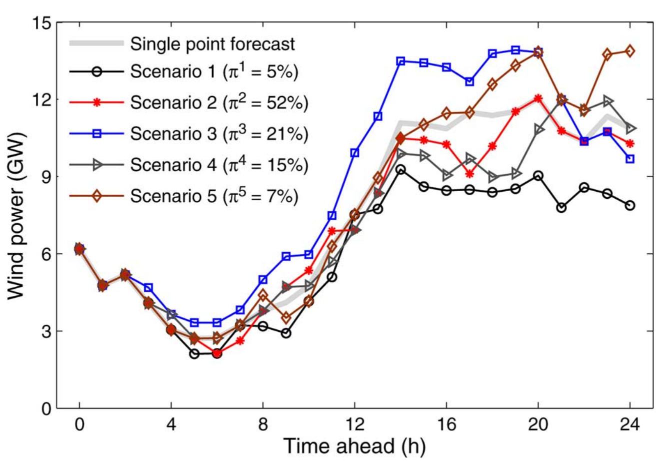

Fig. 10. Probabilistic wind power forecast scenarios and the single point forecast. π^s represents the probability of the sth forecast scenario.

energy generation, over the time horizon, from different technologies for different methods with respect to the results from the PFM are shown in Fig. 14. In the stochastic programming

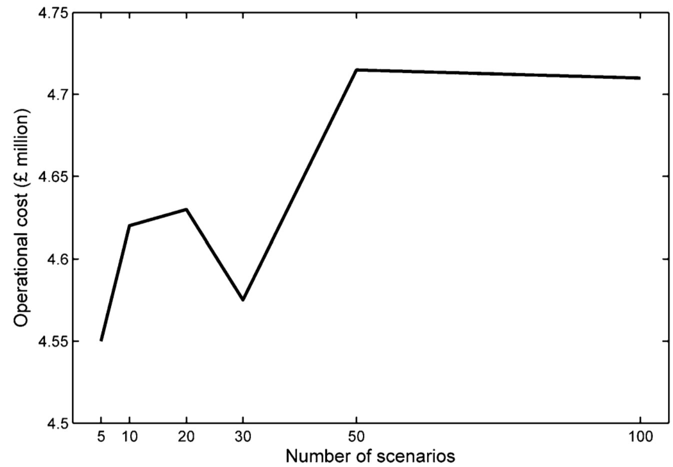

Fig. 11. Comparison between operational cost of the electricity network for different number of forecast scenarios. This comparison was done to test the stability of a scenario reduction algorithm.

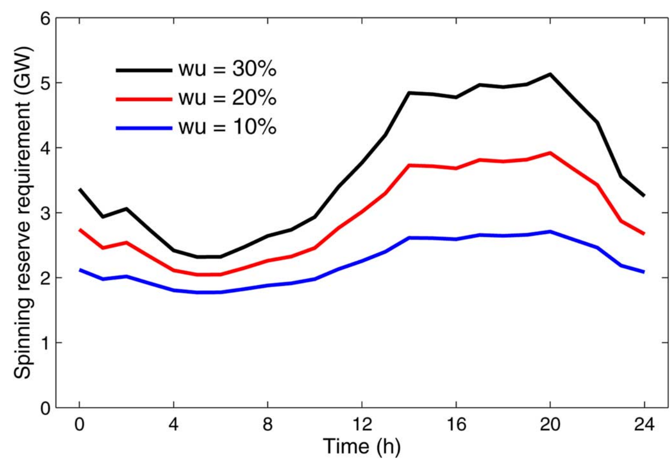

Fig. 12. Spinning reserve requirement for rw = 10%, 20%, and 30%.

TABLE VII
OPERATIONAL COST OF ELECTRICITY NETWORK OVER A DAY FOR rw = 10%, 20%, AND 30%

rw	**10%**	**20%**	**30%**
Operational cost (£million)	33.6	34.3	35.4

methods, the nuclear power plants operate at their maximum capacity over the time horizon. This is due to the lower generation costs of these plants. In the deterministic method, the energy production from nuclear plants was slightly lower than the results from the other methods. Although, the nuclear plants are the cheapest option to meet the demand, more thermal generators came online in order to provide spinning reserve required.

In DM, the electrical energy produced by thermal generation units was less than the output from the same units in the other methods. This is because less energy was consumed by pumped storage plants to fill the reservoirs.

A number of committed thermal units are shown in Fig. 16. In the PFM, fewer units are committed since there is no need to provide reserve to compensate for the uncertainty associated with the wind power forecast.

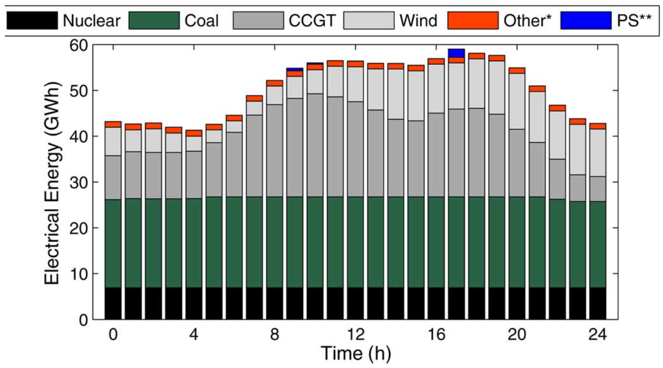

Fig. 13. Power output from different types of generator for the perfect foresight method. * Including Biomass, CHP, and Hydro. ** Pumped Storage.

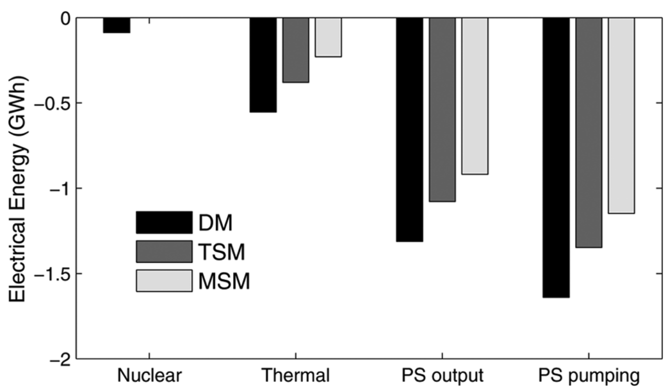

Fig. 14. Changes in expected electrical energy production from different types of generation units in various methods with respect to the energy production in PFM.

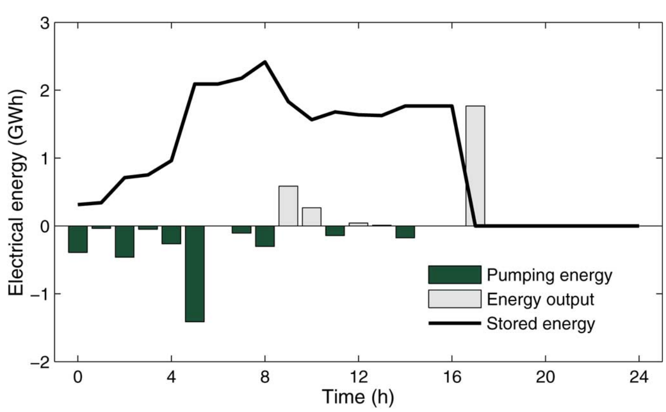

Fig. 15. Total electrical energy used for water pumping, and electrical energy produced by pumped storages units in the PFM.

Provision of spinning reserve capacity to compensate for the uncertainty of wind power forecast resulted in a larger number of committed thermal units in DM. Total electrical energy output, pumping energy, and level of storage for pumped storage plants in the perfect foresight method is shown in Fig. 15.

For the multistage stochastic programming method, there is a unit commitment solution for each forecast scenario (Fig. 17).

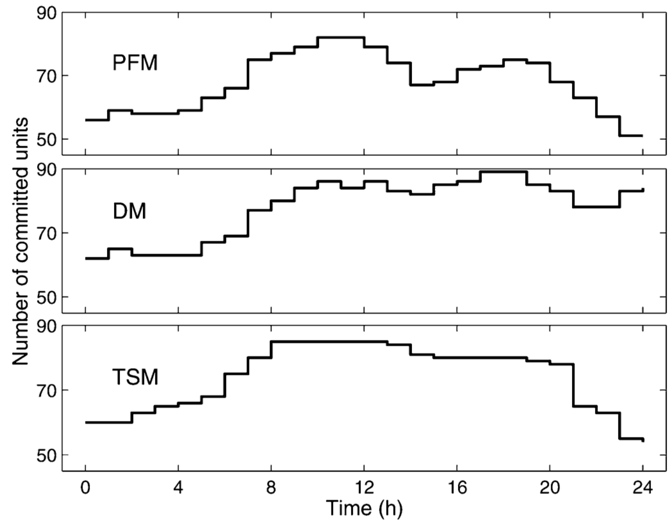

Fig. 16. Number of committed thermal units obtained from PFM, DM, and TSM.

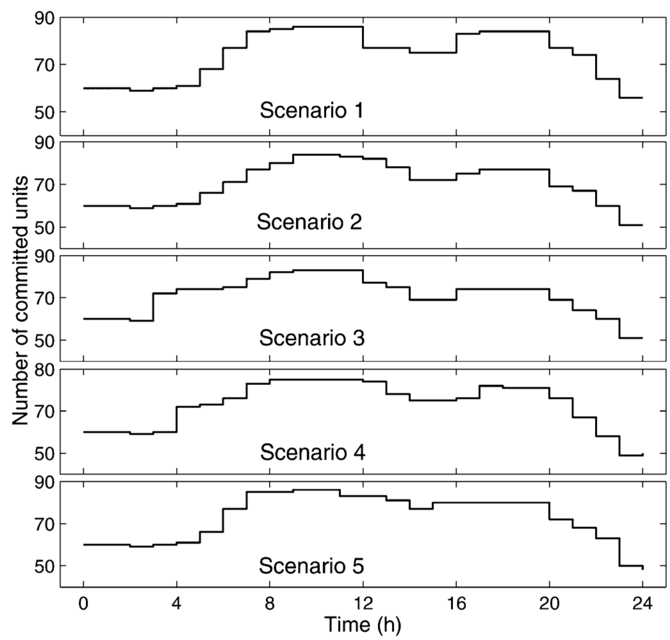

Fig. 17. Number of committed thermal units in various scenarios of the MSM.

C. Gas Network Operation

The analysis of operation of the gas network showed that no load shedding occurred in any of the methods applied. However, in order to deal with the uncertainty of gas demand for power generation, in the deterministic method, higher gas pressure was maintained in the network to increase the linepack [see (27)] and make the network capable of meeting any deviation from the expected gas demand for power generation, locally. The higher pressure of the gas network is the result of the excessive operation of the compressors and has cost implications. The average linepack of the gas network and the total gas consumption by compressors are shown in Table VIII.

TABLE VIII
AVERAGE LINEPACK OF THE GAS NETWORK AND THE TOTAL GAS CONSUMPTION BY COMPRESSORS (MCM)

Methods	Average linepack	Gas consumption by compressors
PFM	307	0.35
DM	318	0.44
TSM	313	0.39
MSM	311	0.36

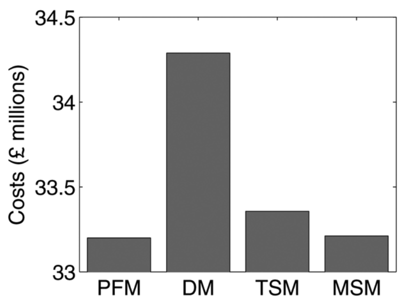

Fig. 18. Operational costs of the electricity network.

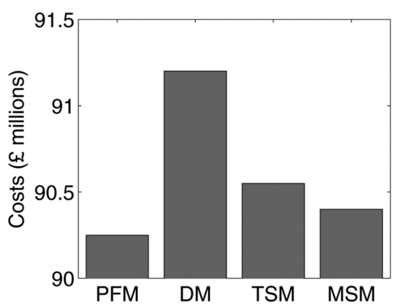

Fig. 19. Total operational costs of the combined network.

TABLE IX
COMPUTATIONAL TIME AND MIP GAP FOR DIFFERENT OPERATIONAL PLANNING METHODS

Methods	PFM	DM	TSM	MSM
Time (sec)	220	1410	243	1156

D. Operational Costs of the Integrated Network

The operational costs obtained from different methods are shown in Figs. 18 and 19, for the electricity network and the integrated network, respectively. Operational cost of the gas network contributed almost 60% of the total cost. In addition to the gas supplied to the gas-fired generators, 275 mcm gas was supplied to the nonpower sectors. The expected value of perfect information (EVPI) was approximated to be equal to $(£)1$ million for DM. The value of the stochastic solution (VSS) for TSM and MSM are $(£)0.7$ million and $(£)0.8$ million pounds, respectively. The operational costs saving due to application of stochastic methods to schedule the GB gas and electricity network was calculated to be at least 255 million pounds in a year.

The computational times for each method are shown in Table IX. The experiments were executed on a laptop with i7-2640M CPU @ 2.80 GHz and 8 GB RAM. The mixed integer programming gap (MIP gap) of 0.8% was achieved in all the methods.

VI. CONCLUSION

Operation of the GB integrated gas and electricity network considering the uncertainty in wind power forecast was investigated using three operational planning methods: deterministic, two-stage stochastic programming, and multistage stochastic programming. These methods were benchmarked against a perfect foresight model which has no uncertainty associated with wind power forecast.

Comparison between the results obtained from different methods showed better performance of the integrated networks occurs when the stochastic programming methods were used. The use of the stochastic methods reduced the operational costs of the gas and electricity networks by almost 1%.

Gas supply constraints to the gas-fired generation units were taken into account through integrating a detailed gas network model to a unit commitment-electricity load flow model. The integrated gas and electricity network was also useful to analyze the impacts of wind forecast uncertainty on performance of the gas network.

The multistage stochastic programming, two-stage stochastic programming, and deterministic methods proposed the least expensive operational strategies for the integrated gas and electricity networks, respectively. The multistage stochastic programming method allows a system operator to improve the unit commitment and economic dispatch decisions at every time step given the constraints link the current state of the systems to the previous' and also take into account the remaining future uncertainties. This characteristic makes this method a useful approach for scheduling thermal generating units and operating the system in a day-ahead and intraday electricity markets.

ACKNOWLEDGMENT

The authors would like to acknowledge the contribution of Dr. H. Hassani, University of Bourmouth, in generating the single forecast of wind power.

REFERENCES

[1] P. Carpentier, G. Gohen, J. C. Culioli, and A. Renaud, "Stochastic optimization of unit commitment: A new decomposition framework," *IEEE Trans. Power Syst.*, vol. 11, no. 2, pp. 1067–1073, May 1996.

[2] J. Wang, M. Shahidehpour, and Z. Li, "Security-constrained unit commitment with volatile wind power generation," *IEEE Trans. Power Syst.*, vol. 23, no. 3, pp. 1319–1327, Aug. 2008.

[3] V. S. Pappala, I. Erlich, K. Rohrig, and J. Dobschinski, "A stochastic model for the optimal operation of a wind-thermal power system," *IEEE Trans. Power Syst.*, vol. 24, no. 2, pp. 940–950, May 2009.

[4] J. Garcia-Gonzalez, R. M. R. de la Muela, L. M. Santos, and A. M. Gonzalez, "Stochastic joint optimization of wind generation and pumped-storage units in an electricity market," *IEEE Trans. Power Syst.*, vol. 23, no. 2, pp. 460–468, May 2008.

[5] F. Bouffard and F. D. Galiana, "Stochastic security for operations planning with significant wind power generation," *IEEE Trans. Power Syst.*, vol. 23, no. 2, pp. 306–316, May 2008.

[6] A. Tuohy, P. Meibom, E. Denny, and M. O'Malley, "Unit commitment for systems with significant wind penetration," *IEEE Trans. Power Syst.*, vol. 24, no. 2, pp. 592–601, May 2009.

[7] K. Methaprayoon, C. Yingvivatanapong, W. J. Lee, and J. R. Liao, "An integration of ANN wind power estimation into unit commitment considering the forecasting uncertainty," *IEEE Trans. Ind. Applicat.*, vol. 43, no. 6, pp. 1441–1448, Nov./Dec. 2007.

[8] M. Qadrdan, M. Chaudry, J. Wu, N. Jenkins, and J. Ekanayake, "Impact of a large penetration of wind generation on the GB gas network," *Energy Policy*, vol. 38, pp. 5684–5695, 2010.

[9] M. Qadrdan, M. Chaudry, J. Ekanayake, J. Wu, and N. Jenkins, "Impact of wind variability on GB gas and electricity supply," in *Proc. 2010 IEEE Int. Conf. Sustainable Energy Technologies (ICSET)*, Kandy, Sri Lanka, 2010.

[10] M. Qadrdan, M. Chaudry, and J. Wu, "Vulnerability analysis of the integrated energy infrastructure," in *Proc. 2009 44th Int. Universities Power Engineering Conf. (UPEC)*, Glasgow, U.K., 2009.

[11] A. Shapiro, D. Dentcheva, and A. Ruszczynski*, Lectures on Stochastic Programming; Modelling and Theory*. Stevenage, U.K.: Pereqrinus Ltd., 1981.

[12] A. J. Wood and B. F. Wollenberg*, Power Generation, Operation, and Control*. Hoboken, NJ, USA: Wiley, 1996.

[13] X. Wang and J. McDonald*, Modern Power System Planning*. New York, NY, USA: McGraw-Hill, 1994.

[14] M. Carrion and J. M. Arroyo, "A computationally efficient mixed-integer linear formulation for the thermal unit commitment problem," *IEEE Trans. Power Syst.*, vol. 21, no. 3, pp. 1371–1378, Aug. 2006.

[15] N. Growe-Kuska, K. C. Kiwiel, M. P. Nowak, W. Romisch, and I. Wegner, "Power management in a hydro-thermal system under uncertainty by lagramgian relaxation," *Decision Making Under Uncertainty: Energy and Power*, vol. 128, pp. 39–70, 2002.

[16] S. Bisanovic, M. Hajro, and M. Dlakic, "Mixed integer linear programming based thermal unit commitment problem in deregulated environment," *J. Elect. Syst.*, vol. 6, pp. 466–479, 2010.

[17] A. Gerber, J. B. Ekanayake, B. Awad, and N. Jenkins, "Operation of the 2030 GB power generation system," *Proc. ICE, Energy*, vol. 164, pp. 25–37, 2011.

[18] A. Osiadacz*, Simulation and Analysis of Gas Networks*. : Gulf Publishing Company, 1987.

[19] M. Chaudry, N. Jenkins, and G. Strbac, "Multi-time period combined gas and electricity network optimisation," *Elect. Power Syst. Res.*, vol. 78, pp. 1265–1279, 2008.

[20] S. An, Q. Li, and T. W. Gedra, "Natural gas and electricity optimal power flow," in *Proc. 2003 IEEE PES Transmission and Distribution Conf. and Exposition*, 2003, vol. 1, pp. 138–143.

[21] M. MacDonald, UK Electricity Generation Costs Update, 2010 [Online]. Available: http://www.decc.gov.uk/assets/decc/statistics/projections/71-uk-electricity-generation-costs-update-.pdf

[22] Operating the Electricity Transmission Networks in 2020, Initial Consultation, National Grid plc., 2009 [Online]. Available: http://www.nationalgrid.com/NR/rdonlyres/32879A26-D6F2-4D82-9441-40FB2B0E2E0C/39517/Operatingin2020Consulation1.pdf

[23] 2011 National Electricity Transmission System Seven Year Statement, National Grid plc., 2012 [Online]. Available: http://www.nationalgrid.com/uk/Electricity/SYS/current/

[24] A. Zhigljavsky, "Singular Spectrum Analysis for Time Series," in *International Encyclopedia of Statistical Science*. New York, NY, USA: Springer, 2011, pp. 1335–1337.

[25] G. Giebel, P. Sorensen, and H. Holttinen, Forecast Error of Aggregated Wind Power, Riso National Laboratory, 2007.

[26] H. Brand, E. Thorin, and C. Weber, "Scenario Reduction Algorithm and Creation of Multi-Stage Scenario Trees," presented at the OSCOGEN, 2002, Discussion Paper No. 7.

[27] J. Dupacova, N. Growe-Kuska, and W. Romisch, "Scenario reduction in stochastic programming: An approach using probability metrics," *Math. Program.*, ser. A 95, pp. 493–511, 2003.

[28] T. Y. Lee, "Optimal spinning reserve for a wind-thermal power system using EIPSO," *IEEE Trans.Power Syst.*, vol. 22, no. 4, pp. 1612–1621, Nov. 2007.

[29] D. Anderson, Power System Reserves and Costs With Intermittent Generation, UKERC Working Paper, 2006.

Meysam Qadrdan (M'13) received the B.Sc. degree in physics from Ferdowsi University of Mashhad, Iran, the M.Sc. degree in energy systems engineering from Sharif University of Technology, Iran, and the Ph.D. degree in electrical engineering from Cardiff University, U.K., in 2005, 2008, and 2012, respectively.

Currently, he is a research associate at the Institute of Energy, Cardiff University. His research looks at energy systems modeling, operational planning of combined gas and electricity networks under uncertainty, and the impacts of wind integration on the operation of power systems.

Jianzhong Wu (M'06) received the Ph.D. degree from Tianjin University, China, in 2004.

He is a Senior Lecturer at the Institute of Energy, Cardiff School of Engineering, Cardiff, U.K. Prior to this, he was a Research Fellow at the University of Manchester, U.K., from 2006 to 2008. He researches power system analysis and control, smart grid, and energy infrastructure.

Dr. Wu is a member of IET and ACM.

Nick Jenkins (M'94–SM'97–F'05) joined Cardiff University, U.K., as a Professor of renewable energy in 2008. From 1992 to 2008, he was at the University of Manchester (UMIST), U.K. Before moving to academia, his career included 14 years of industrial experience. From 2008 to 2011, he was the Shimizu Visiting Professor at Stanford University, USA.

Prof. Jenkins is a Fellow of the IET and the Royal Academy of Engineering and a distinguished member of CIGRE.

Janaka Ekanayake (S'93–M'95–SM'02) received the B.Sc. degree in electrical and electronic engineering from the University of Peradeniya, Sri Lanka, in 1990, and the Ph.D. degree in electrical engineering from the University of Manchester, Institute of Science and Technology, U.K., in 1995.

Since 1992, he has been attached to the University of Peradeniya, and was promoted to Professor of Electrical and Electronic Engineering in 2003. He joined Cardiff University, U.K., as a Senior Lecturer, in 2008, previously being a Research Fellow at the University of Manchester.

Prof. Ekanayake is a Fellow of the Institute of Engineering and Technology, U.K. His main research interests include power electronic applications for power systems and renewable energy generation and its integration.